AFRL-OSR-VA-TR-2013-0153

"Versatile and Robust Software forMulti-Fluid Plasma Modeling"

John Loverich and Uri Shumlak
Tech-X Corporation

April 2013
Final Report

AIR FORCE RESEARCH LABORATORY
AF OFFICE OF SCIENTIFIC RESEARCH (AFOSR)
ARLINGTON, VIRGINIA 22203
AIR FORCE MATERIEL COMMAND

REPORT DOCUMENTATION PAGE

Form Approved
OMB No. 0704-0188

PLEASE DO NOT RETURN YOUR FORM TO THE ABOVE ADDRESS.

1. REPORT DATE *(DD-MM-YYYY)*	2. REPORT TYPE	3. DATES COVERED *(From - To)*
21/01/2013	Final Report	01/03/2012-30/11/2012

4. TITLE AND SUBTITLE

"Versatile and Robust Software forMulti-Fluid Plasma Modeling"

5a. CONTRACT NUMBER

FA9550-12-C-0057

5b. GRANT NUMBER

5c. PROGRAM ELEMENT NUMBER

6. AUTHOR(S)

John Loverich and Uri Shumlak

5d. PROJECT NUMBER

7284

5e. TASK NUMBER

5f. WORK UNIT NUMBER

7. PERFORMING ORGANIZATION NAME(S) AND ADDRESS(ES)

Tech-X Corporation
5621 Arpahoe Ave
Boulder CO 80303-1379

8. PERFORMING ORGANIZATION REPORT NUMBER

Final-72843

9. SPONSORING/MONITORING AGENCY NAME(S) AND ADDRESS(ES)

AF Office of Scientific Research
875 Randolph St Ste 325, RM 3112
Arlington, VA 22203
John Luginsland

10. SPONSOR/MONITOR'S ACRONYM(S)

AFOSR/PKR3

11. SPONSOR/MONITOR'S REPORT NUMBER(S)

AFRL-OSR-VA-TR-2013-0153

12. DISTRIBUTION/AVAILABILITY STATEMENT

Distribution A: Approved for public release; distribution unlimited.

13. SUPPLEMENTARY NOTES

14. ABSTRACT

Tech-X in collaboration with the University of Washington has investigated techniques for improved fully electromagnetic multi-fluid simulation modeling capability on structured and unstructured grids. Among the success of this project include the development of an oracle for predicting the regions of validity of various plasma models, implementation of nodal discontinuous Galerkin methods MUSCL and k-exact finite volume schemes on unstructured meshes for multi-fluid simulations. During the phase I electric field diffusion for divergence cleaning was implemented and demonstrated to work much better than hyperbolic cleaning in the presence of space charge.

Finally, we performed demonstrations of algorithms on complex problems and unstructured domains, including magnetic reconnection and field reversed configuration (FRC) formation.

15. SUBJECT TERMS

STTR PhI, Two-Fluid, Multi-Fluid, FRC, Field Reversed Configuration, High Density Plasma, Discontinuous Galerkin Shock Capturing, Finite Volume, MUSCL.

16. SECURITY CLASSIFICATION OF:			17. LIMITATION OF ABSTRACT	18. NUMBER OF PAGES	19a. NAME OF RESPONSIBLE PERSON
a. REPORT	b. ABSTRACT	c. THIS PAGE			John Loverich
U	U	U	SAR	17	19b. TELEPHONE NUMBER *(Include area code)* 303-996-2029

Reset

Standard Form 298 (Rev. 8/98)
Prescribed by ANSI Std. Z39.18

Final Report on "Versatile and Robust Software for Multi-Fluid Plasma Modeling"

PI: John Loverich, Tech-X Corporation
University Collaborator: Uri Shumlak, University of Washington

Overview

During the Phase I project we were tasked with investigating schemes for multi-fluid plasmas including high order methods on unstructured grids, electric field divergence cleaning, development of multi-fluid benchmarks and the development of an Oracle to tell the user the regimes of validity of various plasma models in a particular simulation. The phase I project was quite successful and details of our progress are described below.

Objectives:

The overall goal of this proposed project (Phase I and II) is to develop a high-fidelity, efficient, accurate and easy-to-use software package for simulation of a broad variety of plasma physics problems relevant to Air-Force applications. Phase I was meant to make progress in this direction.

Status of Effort:

Phase I is finished

Accomplishments/New Findings:

1) Implemented unstructured grid algorithms (DG and finite volume)
2) Added improved implicit schemes for multi-fluid modeling
3) Tested new divergence preservation approach

Publications:

As part of a general description of USim and AIAA paper was presented "Nautilus: A Tool For Modeling Fluid Plasmas", John Loverich, Sean C. D Zhou, Kris Beckwith, Madhusudhan Kundrapu, Mike Loh, Sudhakar Mahalingam, Peter Stoltz, Ammar Hakim. 51st AIAA Aerospace Sciences Meeting including the New Horizons Forum and Aerospace Exposition, 2013, 10.2514/6.2013-1185

This paper gave a general overview of USim (formerly called Nautilus) in its current state including two-fluid and DG algorithms developed during this Phase I project.

Interactions/Transitions:

Many of the two-fluid capabilities developed during this Phase I project will make it to the first release of USim and thus be available to the public.

New Discoveries:

No new discoveries

Honors/Awards:

No awards

Task 1: Create Oracle to Determine validity of models for particular applications

Figure 1 shows the GEM challenge magnetic reconnection problem with the Oracle applied. Colors indicate the regime of validity of each of the plasma models, MHD, Hall MHD, two-fluid and then kinetic models. It's interesting to note how a problem that can essentially be described by two-fluid or Hall MHD initially evolves to something where only kinetic model is strictly valid. The Oracle has been implemented in WarpX and will be implemented in USim during the phase II project.

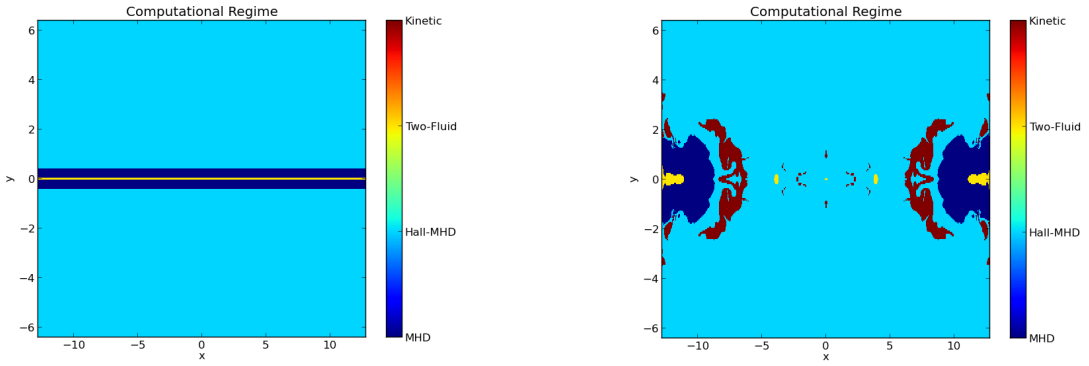

Figure 1: Oracle guides the selection of appropriate physics model which are nested sets, i.e. Kinetic Contains Two-Fluid Contains Hall-MHD Contains MHD. Results applied to the GEM challenge magnetic reconnection problem with nominal values from Earth's magnetosphere identify the simplest, applicable model for the initial and final simulation conditions.

Task 2: Create common geometry and datastructure library for use in both Nautilus and WARPX

Tech-X and UW are currently taking different approaches on the unstructured Grid. Both organizations have finished initial unstructured grid implementations and

algorithms. University of Washington is implementing their grid for GPU and MIC architectures in mind.

This unstructured grid architecture in USim and WarpX allow users to generate custom meshes with increased resolution in areas where small scale effects such as turbulence is expected, or meshes that need to conform to arbitrary geometries. The infrastructure behind mesh generation, conversion, data manipulation and domain decomposition has been largely completed within both codes for 1D, 2D and 3D meshes. Unstructured meshes are currently generated from the mesh generation suite CUBIT in WarpX/M and using Gmsh in USim (addition of CUBIT meshes is occurring as part of a separate project at Tech-X). In WarpX/M Python scripts are used to convert the mesh files and generate initial conditions. The unstructured architecture then imports the mesh and distributes the workload across a compute cluster. Within each cluster node the mesh is further subdivided into patches spread out among compute devices, such as CPUs and GPU's, for processing. The current task is to utilize this infrastructure in the implementation onto the finite volume and finite element methods. Figure 2 shows a flow diagram for the unstructured mesh infdrasturcture in WarpX/M.

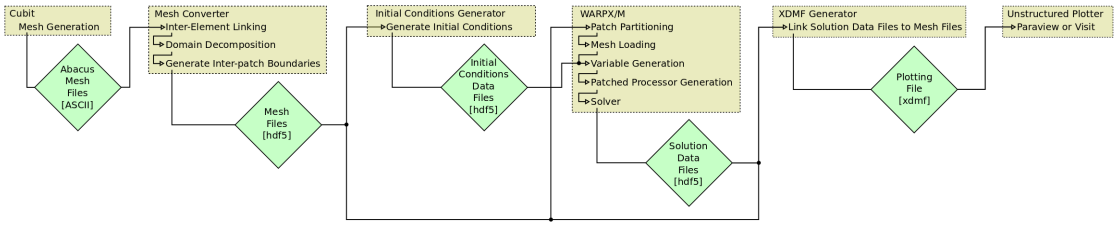

Figure 2: Process diagram of the unstructured mesh infrastructure surrounding WARPX/M. The process starts by designing a mesh within a mesh generation suite (Cubit). The mesh is then converted and read into WARPX/M in which a solution is generated. Solution files are then linked to the mesh file through an xdmf interface file and analyzed in an unstructured data visualizer such Paraview or Visit.

Task 3: Evaluate schemes for efficient robust solution of multi-fluid equations

There are 3 major problems with existing Two-Fluid algorithms used by Tech-X in Nautilus and the UW in Warp-X. (1) a good divergence preserving approach, (2) computational restrictions based on plasma frequency and (3) computational restrictions based on the light speed.

During this project we have implemented a robust solution have resolved problem (2) by using a semi-implicit two-fluid (and 10-moment 2 fluid) algorithm designed by Harish Kumar “Entropy Stable Numerical Schemes for Two-Fluid Plasma Equations” 2012. Harish’s work is similar to previous work performed at the University of Washington however it uses a semi-implicit Runge-Kutta approach that preserves high order time accuracy while being an unsplit scheme. This allows us to resolve issues that we’ve

observed using operator splitting and lower order semi-implicit integration. Furthermore, the approach can be used with Discontinuous Galerkin since it does not require operator splitting. The approach works for both the two-fluid and ten-moment plasma models, and in particular, allows us to use realistic electron masses for FRC and magnetic reconnection simulations.

A very simple multi-dimensional two-fluid test is a ring current formed by strong magnetic field gradients. In this case a magnetic field is embedded in a uniform plasma. The field is positive within a radius of 0.25 and negative otherwise. Conducting walls are used in the domain. The magnetic field gradient generates opposing electron and ion flows and instability quickly develops. We've performed this test on both structured and unstructured grids to help determine the grid dependence of the solution for the finite volume second order MUSCL scheme.

Figure 3 and **Error! Reference source not found.** show solutions on an unstructured grid. The simulations were run on 8 processors. The grid is superimposed on the solution.

Figure 4 and Figure 6 show the solution on a structured grid. The grid clearly plays a role in the final configuration of the solution, however, the basic 4 fold symmetry is captured by the solution on both structured and unstructured grids. It's hoped that by moving to a more accurate algorithm (discontinuous Galerkin) the grid dependence of the solution can be mitigated.

During the Phase I a nodal discontinuous Galerkin method was implemented in 1d and 2d in USim. 1d nodal high order limiters were implemented, but not in multiple dimensions. The DG scheme works extremely well on unstructured grids. Figure 7 through Figure 11 show a simple electromagnetic pulse on an unstructured grid using 3rd order discontinuous Galerkin for Maxwell's equations. The solution shows great uniformity during expansion on the unstructured mesh. We've also demonstrated the nodal DG algorithm on a two-fluid shock in Figure 12 showing that it can be applied to multiple fluids, Maxwell equations and source terms simultaneously. In the current version of the code cell nodal values are averaged to cell centered values for plotting purposes. In the future nodal data will be plotted node by node so that the solution can be seen at the full resolution described by the DG approach.

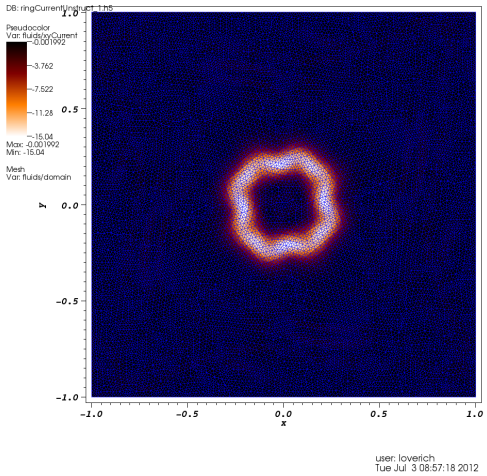

Figure 3: Planar current at time 1 on an unstructured grid. Finite volume scheme.

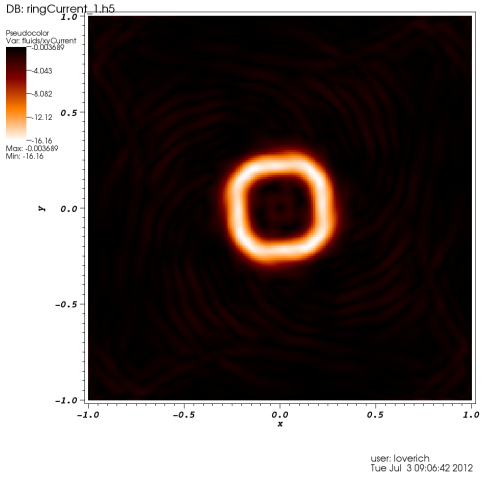

Figure 4: Planar current at time 1 on a structured grid. Finite volume scheme.

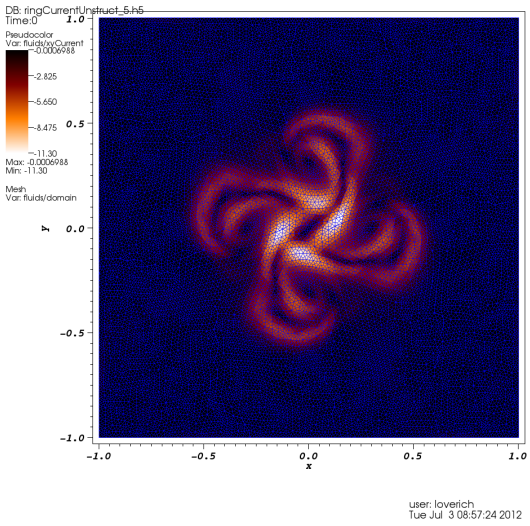

Figure 5: Planar current at time 2 on an unstructured grid. Finite volume scheme.

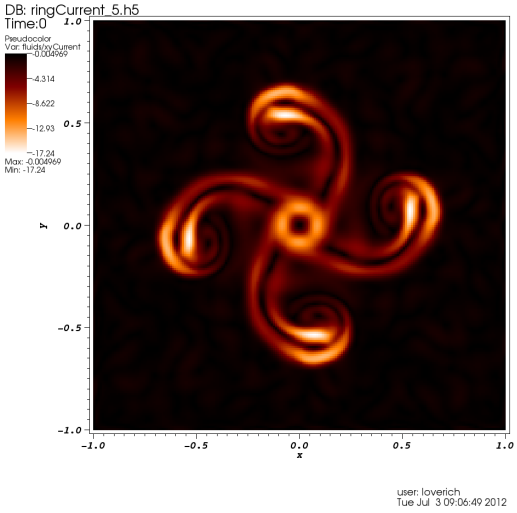

Figure 6: Planar current at time 2 on a structured grid. Finite volume scheme.

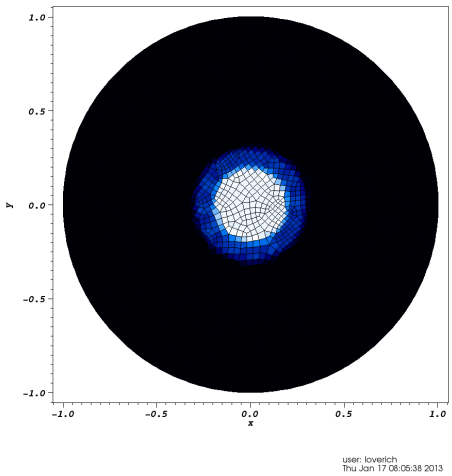

Figure 7: Expansion of electromagnetic pulse time 1. 3rd order nodal DG on unstructured mesh.

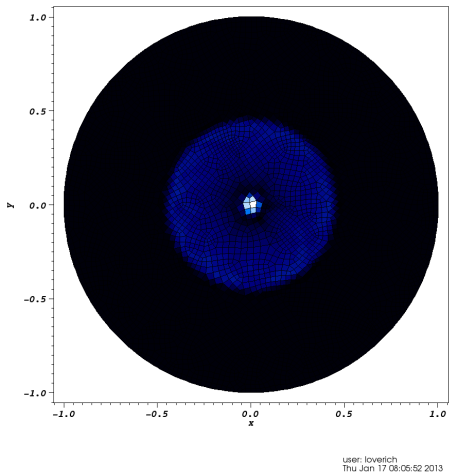

Figure 8: Expansion of electromagnetic pulse at time 2. 3rd order nodal discontinuous Galerkin.

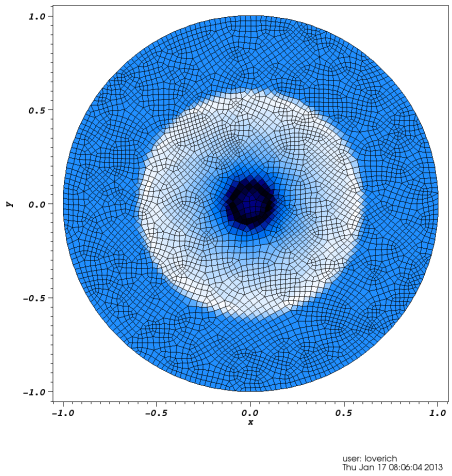

Figure 9: Expansion of electromagnetic pulse time 3. 3rd order nodal discontinuous Galerkin.

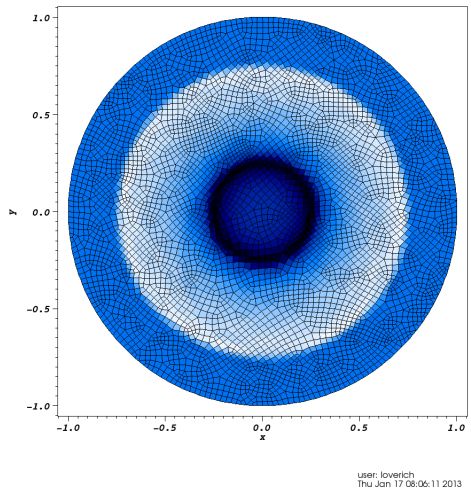

Figure 10: Expansion of electromagnetic pulse time 4. 3rd order nodal discontinuous Galerkin.

Figure 11: Nodal 3rd order discontinuous Galerkin solution for electromagnetic pulse propagation. Nodal values are averaged to cell center for visualization. Results are incredibly uniform despite the unstructured mesh. No limiters were used in this simulation.

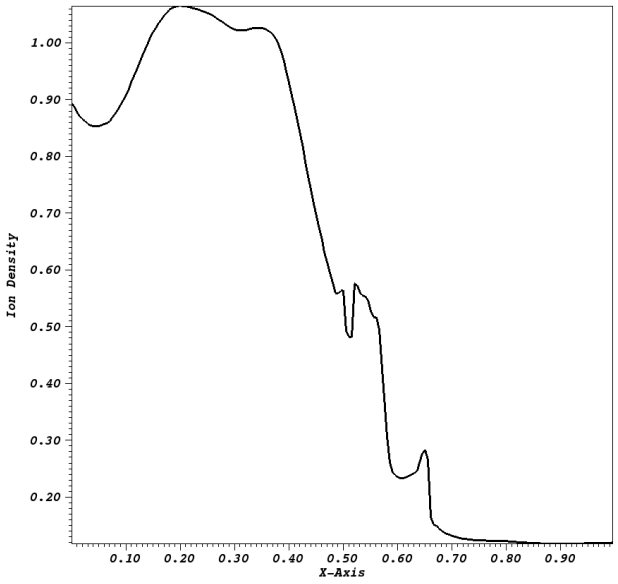

Figure 12: Two-Fluid solution using nodal discontinuous Galerkin method implemented during the Phase I. During the Phase I we implemented 1d and 2d nodal DG without multi-dimensional limiters. No limiters were applied in this case -- however high order nodal limiters are needed in general and would be a part of the phase II project.

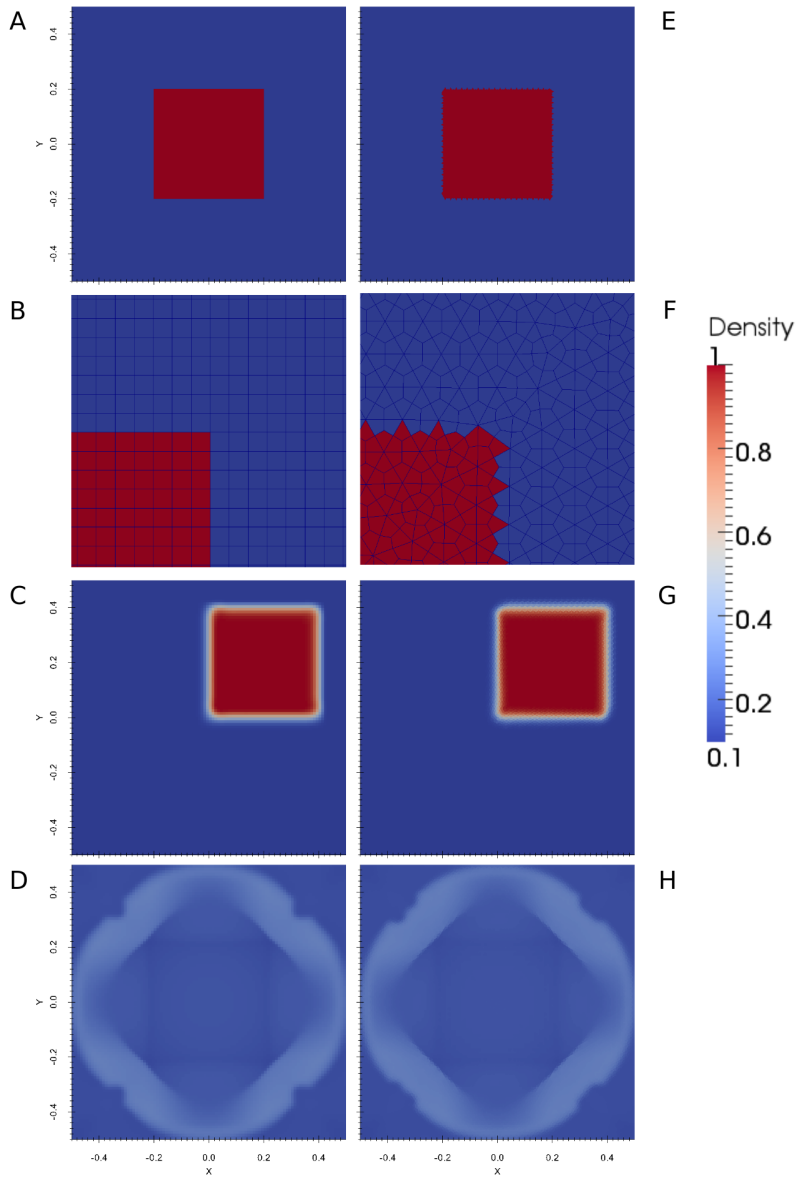

Figure 13: A 2D comparison of a structured grid (left: $\Delta x = \Delta y = 0.01$) and an unstructured meshes (right: $\Delta x_{max} = \Delta y_{max} = 0.01$). Domain size is 1 × 1. (A,E) Initial conditions used for both solvers high density = 1.0 (centered box 0.4 × 0.4) superimposed on low density = 0.1 background). (B,F) Close up view of the initial conditions for the structured grid (B) and unstructured mesh (F). (C,G) Solution to the advection equation (density) at time $t_f = 0.2$ with flow speed of u = v = 1. (D,H) Solution to the Euler equations (density) at time $t_f = 0.2$, with zero initial velocity and constant initial specific internal energy of e = 1.

At the University of Washington the unstructured finite volume method currently under development uses a k-exact polynomial spatial reconstruction in conjunction with a Runge-Kutta time integration scheme. This method allows arbitrary order

accuracy for smooth solutions and drops to 1st order accuracy in the presence of discontinuities. The 1D homogeneous advection, Burger and Euler equations are in working order along with the 2D advection equation. Verification of the 2D Euler equations is currently underway. The unstructured mesh architecture would also be ideal for use with finite element and semi-Lagrange methods. Figure 13 shows advection of a square wave across both a structured and unstructured grid for comparison. The solution shows good shape preservation despite the complex grid structure.

One of the great successes of the Phase I was implementation and testing of diffusion based divergence cleaning of the electric field. Errors in charge conservation are reduced using the equation $\frac{\partial E}{\partial t} - c^2 \nabla \times B = \frac{J}{\varepsilon_0} + \lambda \nabla \left(\nabla \cdot E - \frac{\rho_c}{\varepsilon_0} \right)$ where the last term is the divergence cleaning term. Our previous work with electric field divergence cleaning involved the use of hyperbolic divergence cleaning for the electric field which worked very poorly in cases where there was significant charge separation. During this phase I the parabolic approach was tested on a simple problem (Figure 14) and also tested on more challenging problems such as the GEM challenge problems shown later in this report. Parabolic electric field divergence cleaning was able to maintain small charge separation (small charge conservation error) without destroying the solution. Much more testing of this approach is still needed and that will be pursued during the Phase II project.

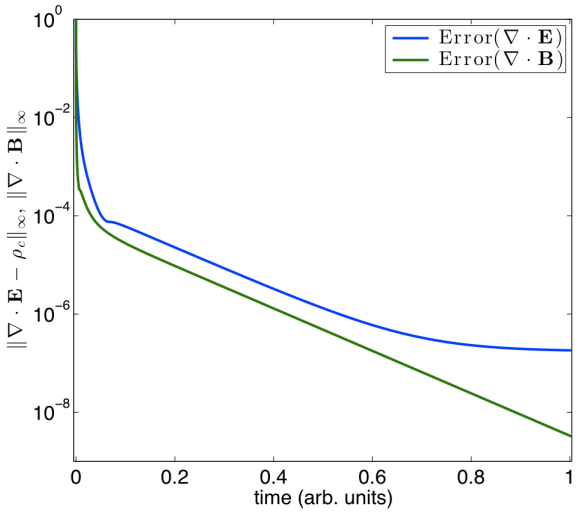

Figure 14: Parabolic cleaning method shown 1D where the magnetic and electric fields are initialized with random noise added to their solution. Results show the monotonic reduction of the divergence error of the magnetic and electric fields.

Task 4: Investigate techniques for solving chemical rate equations implicitly

We've investigated and implemented a Newton iteration combined with high order Runge-Kutta for generic stiff source terms including chemical reactions and multi-fluid momentum and energy exchange terms. Testing is ongoing and will likely be finished as part of the Phase II of this project or through separate funds.

Task 5: Create test suite of problems for verification and validation

During the Phase I we pursued verification and validation tests for the new semi-implicit time integration scheme. Using this scheme we were able to obtain results using realistic electron to ion mass ratio while maintaining high temporal accuracy for FRC formation and magnetic reconnection.

One of the more challenging problems is FRC formation in axisymmetric geometry. Initial conditions for this simulation were provided by Richard Milroy at the University of Washington. Table 1 through Table 4 show results of 5 moment two-fluid FRC formation using realistic electron to ion mass ratio. In order to get the simulations to complete on time we dropped the speed of light by a factor of 100, though running these simulations with the exact speed of light is quite possible. In order to run the simulation we first approximated coil fields by running our Maxwell's equation solver to a quasi-steady state (no interaction between fluids and fields), at which point the full two-fluid simulation began. The FRC chamber is initially filled with an ionized gas at 2ev with a sinusoidal field applied at the boundary and crowbar at 40 microseconds. Table 1 shows the solution near the point where the EM field reaches steady state, just as the two-fluid simulation is turned on. Table 2 shows the solution as the field reverses on the boundary and the plasma is pushed towards the axis and begins to collapse towards Z=0. Table 3 shows the solution at 28 microseconds while the FRC is still compressing and collapsing. Table 4 shows the solution at crowbar and the FRC has reached a relative steady state. We've attempted these same simulations with 10-moment ions, but no success so far. We may still need to work out issues with the axisymmetric source terms – however, we believe simulations in 3D (instead of axisymmetric geometry) with 10 moment ions would probably work.

Table 1: FRC at 6.4 microseconds

Z magnetic field

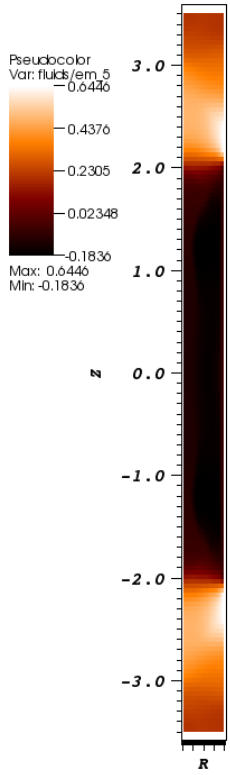

Magnetic field lines

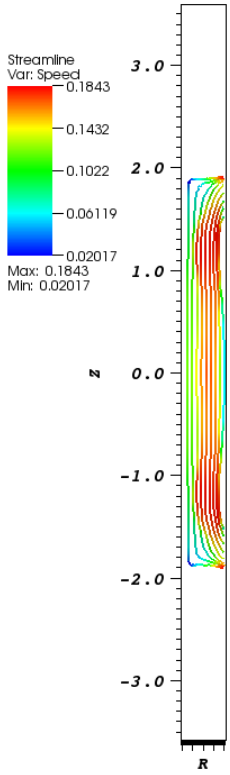

Electron number density

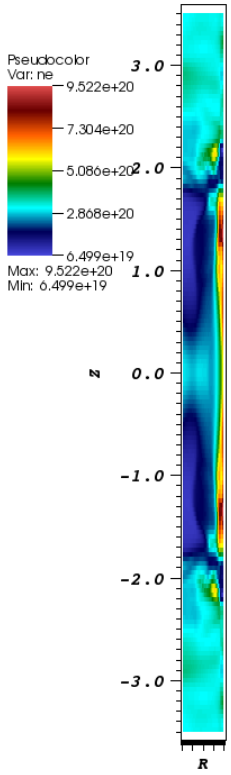

Table 2: FRC at 16 microseconds

Z magnetic field

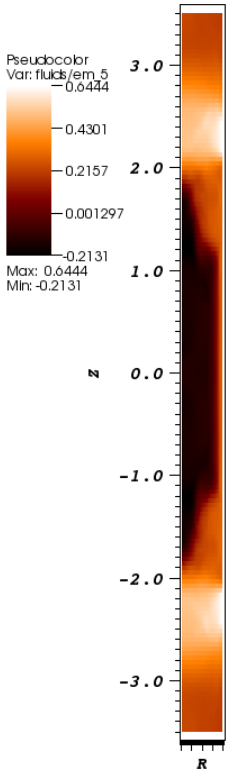

Magnetic field lines

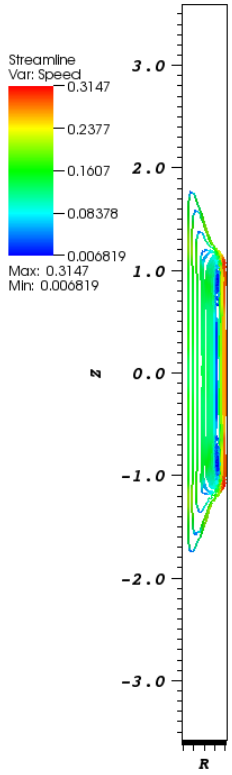

Electron number density

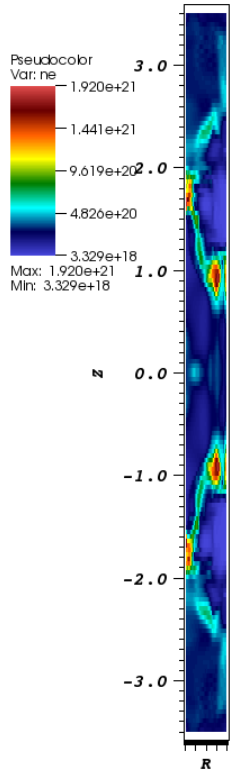

Table 3: FRC at 28 microseconds

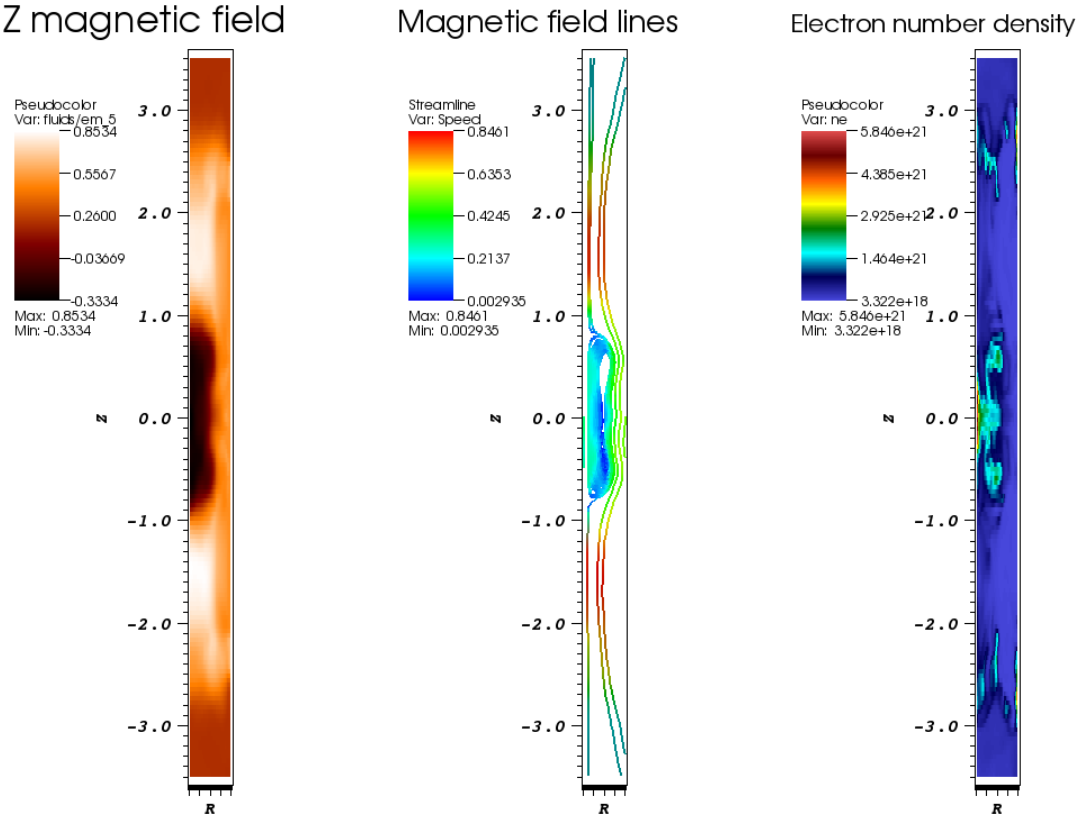

A very common problem for testing two-fluid effects is the GEM challenge magnetic reconnection problem. These simulations were performed with both 5 moment two-fluid and 10 moment ions with 5 moment electrons. There is one key distinction between the two models during magnetic reconnection, i.e. the transfer of kinetic energy to thermal energy. With 10 moment the kinetic energy of reconnection is preferentially transferred to Pxx, the ion pressure in the X direction. Using 5 moment ions it's assumed that Pxx, Pyy and Pzz are equal so the energy is also transferred into the Y and Z components of the pressure tensor. The result is that in the 10 moment simulations we see less expansion of the plasmoids in the y direction as Pyy remains smaller than in the 5 moment ion case. These simulations were performed using the new semi-implicit scheme with realistic electron to ion mass ratio and serve as a verification test of our algorithm for both the 5 moment and 10 moment models in 2D. Figure 15, Figure 16, Figure 17 show the 5 moment solution at various times. Figure 18 and Figure 19 show the 10 moment solutions as various times. Figure 20 shows the reconnected flux for both the 10 moment and 5 moment solutions. In the 5 moment solution magnetic island formation is observed, the island then merges with the main island. After island merger reconnection rates from both the 10 moment and 5 moment solutions agree.

Table 4: Frc at 40 microseconds

Z magnetic field

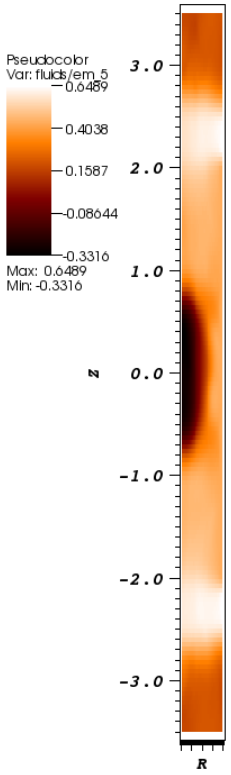

Magnetic field lines

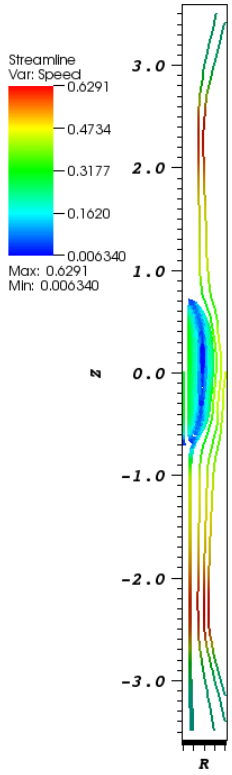

Electron number density

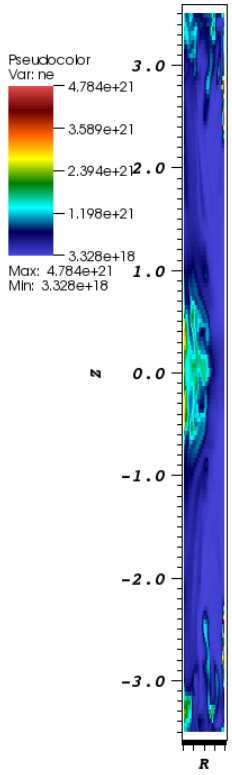

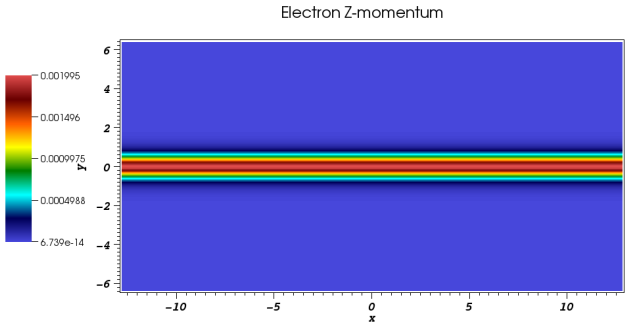

Figure 15: Electron Z-momentum for 5 moment two-fluid reconnection at time 0.

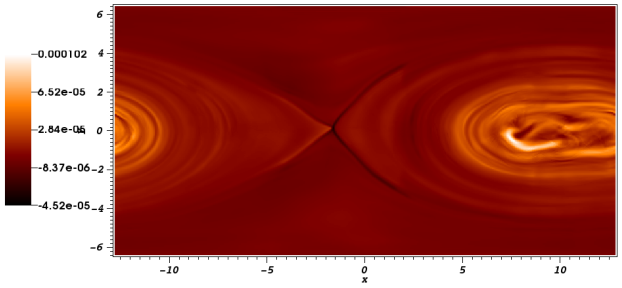

Figure 16: Electron Z momentum for 5 moment two-fluid reconnection at 30 ion cyclotron periods using realistic electron to ion mass ratio.

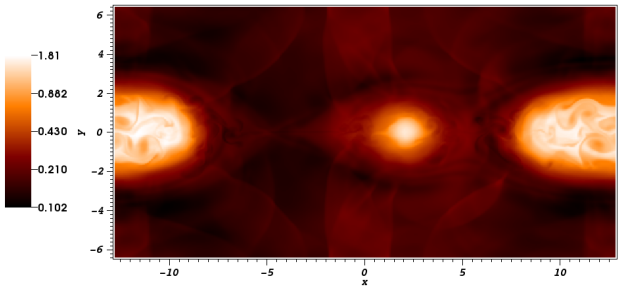

Figure 17: Ion density for 5 moment two-fluid reconnection at 20 ion cyclotron periods using realistic electron to ion mass ratio.

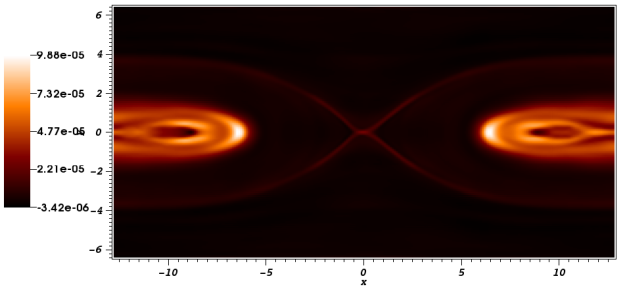

Figure 18: Electron Z momentum for 10 moment two-fluid reconnection at time 30 ion cyclotron times using realistic electron to ion mass ratio.

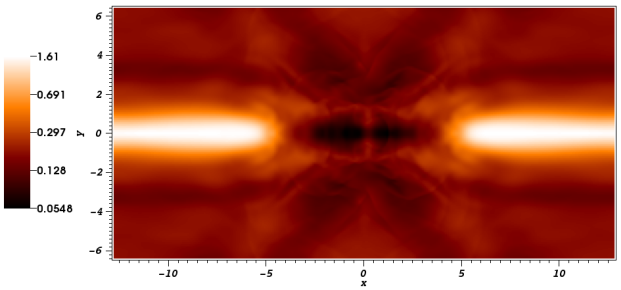

Figure 19: Ion density for 10 moment two-fluid reconnection at time 20 ion cyclotron periods using realistic electron to ion mass ratio.

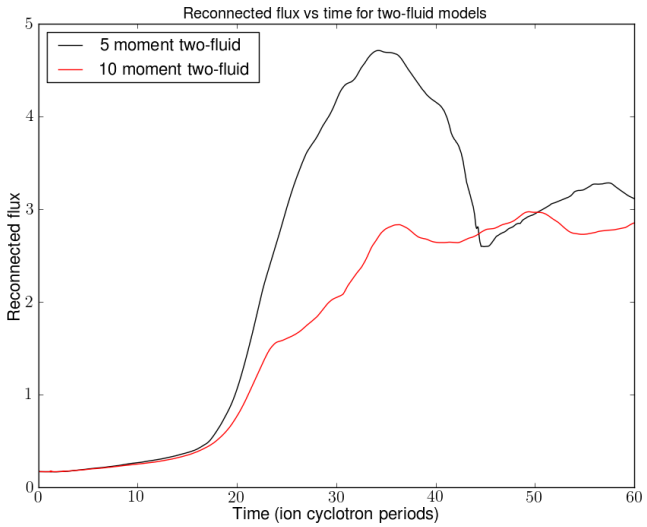

Figure 20: Reconnected flux using 5 moment and 10 moment models with realistic electron to ion mass ratio.